Logistic Sigmoidal and Neural Network Modeling for COVID-19 Death Waves

Oliver Amadeo Vilca Huayta
Departamento de Ingeniería de Sistemas, Universidad Nacional del Altiplano, Peru
E-mail: ovilca@unap.edu.pe

Keywords: Brazil, COVID-19, death number, Italy, logistic sigmoidal model, pandemic, Peru, Switzerland, artificial neural networks

Received: March 3, 2025

The rapid spread of the pandemic of the coronavirus disease 2019 (COVID-19) has caused enormous problems and many deaths. Therefore, it is essential to construct epidemiological models for forecasting and prevention. The main objective of this study is to develop a novel model $F(x)$, treating the cumulative number of deaths due to COVID-19 using two approaches: the logistic sigmoidal function and an artificial neural network. In addition, to estimate models for the death rate $F'(x)$. The research is longitudinal. Data were downloaded from Johns Hopkins University for four countries. It is shown that the logistic function is efficient within the basic sigmoidal functions, and a new variant of the function is obtained and used. The contribution of this work is the model that can be used on data that are not necessarily epidemiological and with any function, where, as x approaches positive and negative infinity, the function tends to a constant value. Also, the method of its construction and the calculation of high-order derivatives allow for the development of a practical model, as well as justification of the term "Wave(s)". The turning points (i.e., the place where the concavity changes) are also obtained and confirmed. Finally, they were applied to real-world datasets. The sigmoidal models yielded better fits than previous works with Pearson correlation coefficients of 0.99992 in Italy, 0.99993 in Brazil, 0.99992 in Switzerland, and 0.99991 in Peru; on the other hand, the Neural Networks reported root mean square errors of 0.0252, 0.0176, 0.0226, and 0.0132, respectively. The models are representative and predictive; they are helpful to understand the pandemic and improve future public health responses.

Povzetek: Prispevek predstavi novo sigmoidalno in nevronsko mrežno modeliranje COVID-19 smrti v štirih državah s ciljem natančnega napovedovanja in razumevanja epidemičnih valov.

1 Introduction

The coronavirus disease 2019 (COVID-19) is highly contagious disease that has caused a high number of deaths and continues to damage the economy and society, to name just a few of its impacts. On October 4, 2024, the Heads of the International Monetary Fund (IMF), the World Bank Group (WBG), and the World Health Organization (WHO) have agreed on broad principles for cooperation on pandemic preparedness (https://www.imf.org; accessed on 7 October 2024). The development and study of epidemiological models can be essential to prevent, predict, or mitigate future epidemics or pandemics. They are also necessary for decision-making, for example, allowing public health institutions to take reliable measures to preserve people's lives [1, 2]. In addition, comparison between countries is considered essential for the control of COVID-19 [3].

In this study, four countries were selected for the purposes of modeling, comparison, and research, namely, Italy, Brazil, Switzerland, and Peru, for which COVID-19 has resulted in a total of 188,322, 333,188, 14,210, and 219,539 deaths, respectively, according to the accumulated death time-series of Johns Hopkins University (https://coronavirus.jhu.edu; accessed on 1 January 2024), without considering the deaths registered after the end of the pandemic. The number of deaths and mortality rates vary between countries and, in this work, we demonstrate that they follow a strict sigmoidal behavior typical of epidemics or pandemics.

Due to the definition of its formula $f(x) = a \cdot e^{-e^{b-c\cdot x}}$ (i.e., double exponential), the Gompertz model requires more elementary operations than the most basic sigmoidal functions. Therefore, this research demonstrated that the logistic function is efficient within the basic sigmoidal functions. Given the logistic function's structure and functionality, we recommend its use in future work.

In addition, a new variant of the logistic function was adapted and obtained, which was called the logistic2 function or simply the logistic function $g(x) = \frac{H}{1+2^{A-Bx}}$, which does not lose any of the original function's properties or qualities. Furthermore, both functions are equivalent.

One of the significant contributions of this work is the model and its construction method. Each function $g(x)_i$ corresponds to wave i. It has the following characteristics or advantages: It does not require any form of integration or union of functions, does not need preliminary work, and it does not require the addition of a dummy variable to the data (or to the function) as in previous works [4, 5]. Mainly

Table 1: Main differences in relation to the key publication

In this work	In Key publication
Estimating any horizontal turning point as a preliminary procedure to obtain $F(x)$ is unnecessary.	Calculating the horizontal turning points is necessary.
The logistic sigmoidal function was used.	The Boltzmann sigmoidal function was used.
A model F was obtained, whose elements are extended to functions that are not necessarily sigmoidal, with $\lim_{x\to-\infty} h(x) = L$ and $\lim_{x\to\infty} h(x) = R$, where L and R are constants. Finally, it was demonstrated with mathematical induction. It was applied to four case studies, where the Peruvian model is: $F(x) = \frac{85.94}{1+2^{6.07-0.048*x}} + \frac{114.1}{1+2^{15.96-0.041*x}} + \frac{13.22}{1+2^{44.35-0.063*x}} + \frac{3.4}{1+2^{73.16-0.082*x}} + \frac{3.33}{1+2^{46.8-0.045*x}}$	The Peruvian model is: $F(x,q) = \frac{(2-q)(3-q)(4-q)(5-q)}{24}\left\{\frac{88.05}{1+e^{\frac{(128.95-x)}{30.88}}}\right\} - \frac{(1-q)(3-q)(4-q)(5-q)}{6}\left\{\frac{113.13}{1+e^{\frac{(390.65-x)}{34.36}}} + 86.49\right\} + \frac{(1-q)(2-q)(4-q)(5-q)}{4}\left\{\frac{14.18}{1+e^{\frac{(698.06-x)}{26.51}}} + 199.34\right\} - \frac{(1-q)(2-q)(3-q)(5-q)}{6}\left\{\frac{3.61}{1+e^{\frac{(898.54-x)}{17.99}}} + 213.37\right\} + \frac{(1-q)(2-q)(3-q)(4-q)}{24}\left\{\frac{2.84}{1+e^{\frac{(1039.82-x)}{25.42}}} + 216.95\right\}$
$\rho = 0.999905$ (the largest). The vertical turning points and higher-order derivatives were calculated.	$\rho = 0.999$. The vertical turning points and higher-order derivatives were not calculated.

for this reason and the previous ones, it is more efficient:

$$F(x) = \sum_{i=1}^{n} \frac{H_i}{1 + 2^{A_i - B_i x}}$$

Where $F(x)$ is the expected cumulative number of deaths, x is the number of days since the first case, n is the number of waves, $1 \leq i \leq n$, H_i is the height of the wave i, A_i and B_i are constants related to the pandemic.

The main objective of this study is to develop a novel and efficient model $F(x)$, treating the cumulative number of deaths due to COVID-19 since the pandemic began as a variable, using the logistic function. Furthermore, artificial neural networks (ANNs) are used, which constitute an alternative method, as machine learning has shown powerful results for studying COVID-19 [6, 7, 8].

The first derivative is calculated to explain the death rate and the magnitude of the COVID-19 waves, where even its graph represents the considered characteristics. In this way, justification is provided for the denomination of COVID-19 "waves." Next, the second derivative is used to calculate the vertical turning points (i.e., the point where the sigmoidal function changes from concave upward to concave downward). At this point, only one last issue remains: the second derivative can report false turning points. Therefore, the turning points are confirmed using the third derivative. Using high-order derivatives—specifically, the first three—allows for an elegant and irrefutable mathematical analysis of any model. Then, the proposed model is applied to four representative countries, yielding novel results.

The differences between the ANN and sigmoidal models were minimal. The ANN's disadvantage is the calculation time.

This paper is structured as follows: Section 2 describes related works, Section 3 presents the materials and methods, and describes the used data. Section 4 demonstrates the results, including those related to the ANN model, the coupled model, high-order derivatives, and the case study, while Section 5 discusses the findings and previous work. Finally, the conclusion is presented in Section 6.

2 Related works

Concerning key publications: While one study has focused on the Peruvian case, it was limited to calculating a function with the Gompertz model and did not apply ANNs. It was carried out with incomplete data as it was conducted during the pandemic period [4]. There is also a study in which $F(x)$ was calculated using the Boltzmann sigmoidal function for a case study (Peru), which was correlated with the social isolation measures in Peru (qualitative variable) [5]; Table **??** illustrates the main differences.

Regarding ANN, several works have used artificial neural networks for prediction. Research has been carried out in India on the Multilayer perceptron [9]. In the United States and India, various artificial neural networks have been used with data on confirmed infections and deaths from COVID-19, of which the convolutional LSTM stood out, which had greater precision and a lower error [10]. In Brazil, a long short-term memory (LSTM) model has been used [11]. Additionally, in China and other countries, it has been concluded that ANNs are adequate to predict global infections and deaths due to COVID-19 [12]. Finally, there is a study in Turkey [13] and in Ada County (Idaho) [14]. A total of six studies were included. The studies were published between 2020 and 2024. Table 2 summarizes the key characteristics of the included studies, detailing the year, countries with metrics (i.e., Pearson correlation coefficient or MSE), key findings, and limitations.

There have not been many related studies on using the logistic sigmoidal function to analyze pandemics. One study

Table 2: Summarizes the six studies included in the review (ANN). It shows the authors, publication year, countries - metrics, key findings, and limitations.

Author	Year	Countries and metrics	Key findings and limitations
Sujath, R. et al. [9]	2020	Pearson correlation: $\rho_{India} \approx 0.968$ confirmed deaths	Feedforward artificial neural network (FANN). They worked with preliminary data (two months).
Shastri, Sourabh et al. [10]	2020	It does not present correlation coefficients. They use Mean Absolute Percentage Error (MAPE) for India and USA	Long short-term memory. They worked with preliminary data (approximately four months) and presented a comparative study of the two countries' results (India and USA).
Fernandes, Filipe et al. [11]	2022	Pearson correlation: $\rho_{Brazil} \approx 0.9826$, $R^2 = 0.9656$ for confirmed deaths	Long short-term memory (LSTM) and others. A study was conducted for the State of Santa Catarina, Brazil. Preliminary data was used.
Namasudra, Suyel et al. [12]	2023	Pearson correlation: $\rho_{India} \approx 0.99914$ (Overall performance of death cases)	Nonlinear Autoregressive (NAR) Neural Network Time Series (NAR-NNTS) and others. The study was conducted in India. Preliminary data was used (January 2020 to August 2020).
Özen, Figen et al. [13]	2024	Pearson correlation: $\rho_{Turkey} \approx 0.9917$, $R^2 = 0.9834$ (daily deaths)	Random forest regression and machine learning models (i.e., LSTM and ARIMA). The data starts on March 11, 2020 and ends on June 1, 2022 (they do not cover until the end of the pandemic). The study was conducted in Turkey.
Kanchan, Swarna et al. [14]	2024	Pearson correlation: $\rho_{Ada\ County} = 0.669$ (predicted daily deaths)	ANN model. The data cover June 7, 2021, to July 1, 2022 (they do not cover until the end of the pandemic). The study was conducted for the city of Boise (Ada County), the capital of Idaho.

used the extended logistic function in this context [15]; however, the authors did not compare it with an ANN, and did not calculate derivatives or turning points. Similarly, in Mexico, the Gompertz function was used [16], and in Brazil and other countries, the Boltzmann function was used [17]. A total of five studies were included detailing each method's performance metrics. The studies were published between 2021 and 2024. Table **??** summarizes the key characteristics of the included studies.

3 Materials and methods

3.1 Dataset

The database of the total number of deaths used in the current study is publicly available (open access) from the Coronavirus Disease Data Repository of Johns Hopkins University (https://github.com/CSSEGISandData/COVID-19; accessed on 1 January 2024). Complete data for different countries are also available [18].

No data preprocessing was necessary, as there were no missing or outlier data; only the data from the countries under study were selected. Normalization (using the mean and standard deviation) was applied for the artificial neural networks.

The study would be trivial with data from the first days of the pandemic. For example, in Peru and most countries, during the first 20 days, the curve barely begins to grow and can be fitted to an exponential or even linear model. In contrast, a model is required for the complete dataset (from the beginning to the end of the pandemic). Moreover, modeling a single wave can be relatively easy [19].

In this work, no function integration method is required [4], and a program is used to process and estimate F.

3.2 The sigmoidal logistic function

The sigmoidal logistic function can be applied to a time-series [20]. It has different applications, such as representing epidemic curves. It is represented by the following function:

$$g\left(x\right) = \frac{H}{1 + \mathrm{e}^{A - Bx}}, \tag{1}$$

Where x is the number of days since the first case, $g(x)$ is the expected cumulative number of deaths, H is the height of the wave, A and B are constants related to the pandemic, and e is a mathematical constant (i.e., an irrational and transcendental number approximately equal to 2.718281828459045).

In this work, a new version of the logistic function is used, which we call the logistic2 function or, simply, the logistic function:

Table 3: Summarizes the five studies included in the review (sigmoidal functions). It shows the authors, publication year, countries - metrics, key findings, and limitations.

Author	Year	Metrics	Key findings and limitations
Abolmaali, Saina et al. [15]	2021	MSE: US=678.7, India = 631.3, Brazil=731.0, and Russia = 1501.1	Logistic regression and other models were used. They worked with preliminary data (approximately one year). No correlation coefficients were provided. Finally, the model is simple (a single sigmoidal function).
Conde, R. et al. [16]	2021	Pearson correlation: $\rho_{Mexico} \approx 0.9998$	The Gompertz sigmoidal function was used. Preliminary data (one wage or six months) was used during the pandemic. The model is simple and for a single wave.
Vilca, Oliver et al. [4]	2023	Pearson correlation coefficient: ρ_{Peru} = 0.9577994	The Gompertz sigmoidal function was used. It requires inserting a dummy variable q into the model and the database. Data available at that time (up to the third wave) was used. The models: $F(x,q) = \sum_{w=1}^{n} \left(\frac{\prod_{i=1}^{w-1}(i-q)\prod_{j=w+1}^{n}(j-q)}{(n-w)!(-1)^{w-1}(w-1)!} \cdot A_w \cdot e^{-e^{B_w - C_w \cdot x}} \right)$ $F(x,q) = \sum_{w=1}^{n} \left(\frac{2^{w-1}\&q}{2^{w-1}} \cdot A_w \cdot e^{-e^{B_w - C_w \cdot x}} \right)$ Where A_w, B_w, and C_w are constants related to the pandemic.
El Aferni, Ahmed et al. [17]	2023	$\rho_{United\ Kingdom} \approx 0.99912$ $\rho_{Zambia} \approx 0.9991$ $\rho_{Brazil} \approx 0.9995$ $\rho_{South\ Africa} \approx 0.999925$	The sigmoid Boltzmann model was found to be effective in fitting the cumulative number of COVID-19. With data covering up to the fourth wave. The model is: $F(x) = I_{min} + I_{max} \sum_{i=1}^{n} \left(\frac{P_i}{1+10^{(A_i - x)B_i}} \right)$, where P_i, A_i, B_i, I_{min} and I_{max} are constants related to the pandemic.
Vilca, Oliver et al. [5]	2024	Pearson correlation coefficient: ρ_{Peru} = 0.999	The Boltzmann sigmoidal function was used. Performed with complete data. It requires the insertion of a dummy variable q in the model and the database. The models: $F(x,q) = \sum_{w=1}^{n} \left(\frac{\prod_{i=1}^{w-1}(i-q)\prod_{j=w+1}^{n}(j-q)}{(n-w)!(-1)^{w-1}(w-1)!} \frac{I_w}{1+e^{\frac{(Z_w - x)}{D_w}}} \right)$ $F(x,q) = \sum_{w=1}^{n} \left(\frac{2^{w-1}\&q}{2^{w-1}} \frac{I_w}{1+e^{\frac{(Z_w - x)}{D_w}}} \right)$ where I_w, Z_w and D_w are constants related to the pandemic.

Note: $F(x)$ and $F(x,q)$ are the expected cumulative number of deaths, x is the number of days since the first case, and n is the number of waves.

$$g(x) = \frac{H}{1 + 2^{A-Bx}}, \tag{2}$$

where A and B are new pandemic-related constants. Instead of the irrational number e (which cannot be expressed as a fraction m/n, where $m, n \in \mathbb{Z}$), we use the natural number 2 as, in computing, we can efficiently calculate 2^k if $k \in \mathbb{N}$.

The high-order derivatives were calculated by hand and checked using Octave Software (version 9.1.0). This approach improved the factorization and presentation of the functions

3.3 Software and hardware

For all models, the same computer, operating system, and programming language were used:

1. HP 11th Generation Intel(R) Core™ i7-1165G7 2.8 GHz computer. RAM 16 GB.
2. Windows 11 Pro Operating System.
3. The R programming language (version 4.4.1 - free software environment for statistical computing and graphics), and the integrated development environment (IDE) RStudio Desktop (2024.09.0+375 "Cranberry Hibiscus" release).

The algorithm for the logistic model has the following procedures:

1. Load libraries (data structures, nonlinear regression, metrics, graphs, and neural networks).
2. Select country and language.
3. Load data.
4. Estimate the model (providing starting values).
5. Show goodness-of-fit reports (ρ, MAE, RMSE, and p-values).

6. Export the model $F(x)$, the first derivative $F'(x)$, and the second derivative $F''(x)$.

7. Generate the graph (configuring color, size, resolution, and output file, among others).

3.4 Parameter initialization

Parameters of the Logistic Sigmoidal Model: Non-linear regression with numerical algorithms may require initialization parameters. In this case, estimated values were provided. For instance, the approximate height of the sigmoidal function, H, can be obtained by observing the scatter plot (observed data).

Parameters of the ANN Model: The Long Short-Term Memory (LSTM) model was used, considering previous works [10, 11, 13]. It is designed to effectively process and retain information over multiple steps. A single hidden layer is sufficient to simplify the LSTM architecture.

The number of epochs was chosen experimentally (i.e., 500), increasing until an acceptable fit was achieved. Similarly, the ADAM optimizer performed slightly better than RMSProp. The input layer contains one neuron since there is one input (the cumulative number of deaths). Likewise, the output layer contains one neuron as it is a regressor. For the number of neurons in the hidden layer, the following formula was used: $N = \frac{N_s}{\alpha(N_i+N_o)}$, where N_i represents the number of input neurons, N_o the number of output neurons, N_s the number of samples in the training dataset, and α is a scaling factor typically between 2 and 10. With $N_i = 1,\ N_o = 1$, $N_s = 1100$ and $\alpha = 2.75$, the number of neurons is $N = 200$.

3.5 Statistical analyses

For model comparison, three metrics were used. For a sample of n observations y_i ($i = 1, 2, \cdots, n$), and n corresponding model predictions $\hat{y}_i$, where $\bar{y}$ is the mean of the y-values and $\bar{\hat{y}}$ is the mean of the $\hat{y}$-values.

The Pearson product-moment correlation coefficient or Pearson correlation coefficient (ρ for short) is a measure of linear dependence and its direction between two quantitative variables. If there is a positive correlation, when one variable changes, the other variable changes in the same direction; if there is no correlation (zero), there is no relationship between the variables; and, if there is a negative correlation, the opposite of the positive correlation occurs: $\rho = \frac{\sum(y_i-\bar{y})(\hat{y}_i-\bar{\hat{y}})}{\sqrt{\sum(y_i-\bar{y})^2 \sum(\hat{y}_i-\bar{\hat{y}})^2}}$

The root mean square error (RMSE) is the standard deviation of the residuals. Residuals represent the differences between the values that a model predicts and those that are observed: $RMSE = \sqrt{\frac{1}{n}\sum_{i=1}^{n}(y_i - \hat{y}_i)^2}$.

The Mean Absolute Error (MAE) calculates the average absolute difference between predicted and actual values: $MAE = \frac{1}{n}\sum_{i=1}^{n}|y_i - \hat{y}_i|$.

The metrics are complementary and widely used; while ρ measures the strength and direction of the relationship between two datasets, RMSE and MAE measure the difference between them.

A significance test was performed for the Pearson correlation coefficients, and the F-test was used for the sigmoidal models. Concretely, statistics were used to model, analyze, interpret, and present the results.

3.6 Research design

This research is longitudinal, retrospective, and correlational.

This research poses the following question: Do the models fit the cumulative number of deaths? Then, for each model and each country, the hypotheses are:

The logistic sigmoidal model fits the cumulative number of deaths. The F-test is used (at a significance level of 0.01).

The performance scores were used for the ANN. The correlation hypothesis states that a positive and significant correlation exists between the ANN and the accumulated number of deaths (at a significance level of 0.01).

4 Results

This study considers a new model and a simple way to couple sigmoidal functions.

4.1 Case studies

Four countries were intentionally selected; simple random sampling was not used: Italy (Southern and Western Europe), Brazil (South America), the Swiss Confederation (west-central Europe), and Peru (South America).

Table 4 presents specific data for each country (2020): Population, number of deaths, start and end dates of the pandemic (number of days), and the death percentage in relation to the population of each country ($\frac{Deaths}{Population} \cdot 100$). The population data were downloaded from "Population Pyramids of the World" (https://www.populationpyramid.net; accessed on 1 September 2024).

Day one corresponds to the first death. The pandemic began in February 2020 in Italy and in March in Brazil, Switzerland, and Peru. It lasted until 9 March 2023, specifically 1113 days in Italy, 1088 days in Brazil, and 1099 days in Switzerland and Peru.

From Table 4, it can be seen that the country with a considerably higher percentage of deaths, according to the total number of inhabitants, was Peru (0.66%), followed by Italy (0.32%), and ending in a tie between Brazil and Switzerland (0.16%).

These countries differ in location, population, and number of deaths from COVID-19.

Table 4: Data for each country (2020): Population, number of deaths, start and end dates of the pandemic (number of days), and the death percentage in relation to the population of each country.

Country	Population	Number of deaths	Start and end date of the pandemic (number of days)	Percentage of deaths
Italy	59,500,579	188,322	From 21 February 2020 to 9 March 2023 (1113 days)	0.32 %
Brazil	213,196,304	333,188	From 17 March 2020 to 9 March 2023 (1088 days)	0.16 %
Switzerland	8,638,613	14,210	From 06 March 2020 to 9 March 2023 (1099 days)	0.16 %
Peru	33,304,756	219,539	From 06 March 2020 to 9 March 2023 (1099 days)	0.66 %

Table 5: Artificial neural networks adjustment measures.

Country	Pearson Correlation ρ	Coefficient of Determination	RMSE	MAE	p-value for ρ	Confidence interval for ρ	Running time (min)
Italy	0.999715	0.999431	0.0252	0.0162	$< 2.2 \cdot 10^{-16}$	0.9997 , 0.9997	16.698
Brazil	0.999862	0.999724	0.0176	0.013	$< 2.2 \cdot 10^{-16}$	0.9998 , 0.9999	16.239
Switzerland	0.999805	0.99961	0.0226	0.0132	$< 2.2 \cdot 10^{-16}$	0.9998 , 0.9998	16.467
Peru	0.99994	0.999879	0.0132	0.0095	$< 2.2 \cdot 10^{-16}$	0.9999 , 0.9999	16.43
Average	0.999831	0.999661	0.0196	0.013	$< 2.2 \cdot 10^{-16}$		16.458
Std. Dev.	9.4e-05	0.000189	0.0053	0.0028	$< 2.2 \cdot 10^{-16}$		0.188

4.2 Artificial neural networks

In machine learning, a neural network (NN), also called an artificial neural network (ANN), is a model composed of connected units or nodes called neurons [21]. NNs, learn by example, the ANN is set up during a learning process to perform specific tasks, such as identifying patterns and categorizing information [22].

Long short-term memory (LSTM) is a type of recurrent neural network (RNN) architecture designed to address the limitations of traditional RNNs, especially when it comes to learning long-term dependencies. The main innovation of LSTM is the use of gating mechanisms to control the flow of information through the network. This allows the LSTM to maintain and update its internal state over long periods [23, 24].

R provides libraries and frameworks that simplify the process of building and training neural networks, including LSTM networks. The Keras library provides a high-level interface for building and training neural networks. To the authors' knowledge, Python has been used in most previous works.

The LSTM was used with the following characteristics: three layers (1 input neuron, 200 neurons in the hidden layer, and one output neuron), the "adam" optimizer, loss = "mae", epochs = 500, and batch_size = 1 (see section 3.4 for more details).

Table 5 presents the ANN model's goodness-of-fit results by country, as well as the averages and standard deviations. On the one hand, the average RMSE and MAE of the ANNs were quite acceptable (0.0196 and 0.013, respectively, on scaled data; see columns four and five). On the other hand, the Pearson correlation coefficients (ρ) were quite good: Those for Italy, Brazil, Switzerland, and Peru were 0.999715, 0.999862, 0.999805, and 0.99994, respectively (usually varying with each execution).

Moreover, the correlations are statistically significant in the four countries (the p-values are below the significance level of 0.01). In R, p-value $< 2.2e-16$ means that the p-value is less than $2.2 \cdot 10^{-16}$ (scientific notation for 0.00000000000000022). The confidence intervals are presented in column seven.

The correlations (ρ) for the ANN did not differ much because ANNs adapt well to data. However, sigmoidal logistic models require the data to follow a pattern.

For some countries, the data fit better; however, all countries fit pretty well.

The coefficients of determination (third column) indicate that the models obtained are explained or determined by the differences in the days.

In column eight of Table 5, the average empirical execution time per country (measured in minutes) is presented. An experiment consists of measuring the initial time, estimating the model, obtaining the final time, and calculating the difference (the Sys.time() function from R was used). The experiment was repeated forty times [25] in each country, and the average was recorded to avoid bias. The average time is 16.698 minutes in Italy, 16.239 in Brazil, 16.467 in Switzerland, and 16.43 in Peru.

Finally, the source code for the artificial neural networks is presented in Appendix B.

4.3 Calculating the number of operations of sigmoidal functions.

The execution time of a sigmoidal function depends on the type and number of operations. In general, the order of the execution time of the operations, from smallest to largest, is as follows: (1) addition or subtraction, (2) multiplication or

Table 6: Number of operations in sigmoidal functions

Sigmoidal function	**Number of power operations**	**Number of division operations**	**Number of multiplication operations**	**Number of addition or subtraction operations**
Gompertz function: $g(x) = A \cdot e^{-e^{B-D \cdot x}}$	2	0	2	1
Hyperbolic tangent function: $g(x) = tanh(x) = U - \frac{H}{1+e^{2(x-A)}}$	1	1	1	3
Boltzmann function: $g(x) = \frac{H}{1+e^{(C-x)/D}}$	1	2	0	2
Logistic function: $g(x) = \frac{H}{1+\mathrm{e}^{A-Bx}}$	1	1	1	2

division, and (3) exponentiation with a real number in the exponent; that is, addition/subtraction is calculated faster than the other two, and multiplication/division is generally faster than exponentiation.

Then, for evaluation, the following functions are considered: those based on the Gompertz function (representing the double exponential functions), based on the hyperbolic tangent function (representing the extended functions of the logistic function), the Boltzmann function, and the logistic function. The number of operations was calculated, as detailed in Table 6.

Moreover, the execution times were calculated based on the results from Table 6:

$$\begin{aligned} T_{Go} &= M\log(B-Dx) + Mlog(e^{B-Dx}) + 2M + S \\ T_{Hp} &= M\log(2(x-A)) + D + M + 3S \\ T_{Bz} &= M\log((C-x)/D) + 2D + 2S \\ T_{Lg} &= M\log(A-Bx) + D + M + 2S \end{aligned}$$

Where the execution times for the basic operations are as follows: Exponentiation (a^b) requires $\log b$ multiplications, division is D, multiplication is M, and addition/subtraction is S.

The Gompertz function was found to be the least suitable, as it has two exponential operations, two multiplication operations, and one subtraction operation. Meanwhile, the hyperbolic tangent function has an additional subtraction operation in relation to the logistic function. The Boltzmann function has two divisions (generally, in computing, the division operation costs more than multiplication). Finally, the logistic function was selected because it has the simplest operations and in the minimum quantity, considering the set of basic sigmoidal functions. It could barely be equaled by some extended sigmoidal functions and, therefore, it was considered efficient.

4.4 Coupled models or functions

It has the following characteristics or advantages: First, it does not require any form of integration or union of functions, and second, it does not need to add a dummy variable to the data or to the function as in previous publications [4, 5].

Theorem 1. The coupled model (or coupled function) with n sigmoidal logistic functions is:

$$F(x) = \sum_{i=1}^{n} \frac{H_i}{1+2^{A_i - B_i x}} \tag{3}$$

Where $F(x)$ is the expected cumulative number of deaths, x is the number of days since the first case, n is the number of waves ($1 \leq i \leq n$), H_i is the height of the wave i, and A_i and B_i are constants related to the pandemic.

Furthermore, $x_0 < x_1 < x_2 < \cdots < x_n$ are consecutive real numbers that determine the intervals of the logistic functions. The function $g(x)_i$ is defined on the interval $x \in [x_{i-1}, x_i]$; $\forall x > x_i$, $g(x)_i$ tends to H_i, and $\forall x < x_{i-1}$, $g(x)_i$ tends to 0 (limits of the sigmoidal logistic function).

Therefore $\lim_{x\to-\infty} F(x) = 0$ and $\lim_{x\to\infty} F(x) = \sum_{k=1}^{i} H_k$.□

Proof. Let $x_0 < x_1 < x_2 < \cdots < x_n$ be consecutive real numbers determining the intervals of logistic functions. In general, the function $g(x)_i$ is defined on the interval $x \in [x_{i-1}, x_i]$ (the i-th "wave"); $\forall x > x_i$, $g(x)_i$ tends to H_i, and $\forall x < x_{i-1}$, $g(x)_i$ tends to 0 (right and left limits of the sigmoidal function).

Proof by mathematical induction: Base case $F(x)$ with two functions; if $x < x_0$, then $F(x) \approx 0$ (the left-hand limits are zero); if $x \in [x_0, x_1]$, then $F(x) \approx g(x)_1$; if $x \in [x_1, x_2]$, then $F(x) \approx g(x)_1 + g(x)_2 \approx H_1 + g(x)_2$, and if $x > x_2$, then $F(x) \approx H_1 + H_2$.
Induction hypothesis:
$E(x) \approx \sum_{k=1}^{i-1} \left(\frac{E_k}{1+2^{A_k - B_k x}}\right)$, $\forall x \in [x_0, x_{i-1}]$ where $\lim_{x\to-\infty} E(x) = 0$ and $\lim_{x\to\infty} E(x) = \sum_{k=1}^{i-1} H_k$
Inductive step: By definition of $F(x)$,
$F(x) \approx E(x) + g(x)_i$, $\forall x \in [x_0, x_i]$
$F(x) \approx \sum_{k=1}^{i-1} \left(\frac{H_k}{1+2^{A_k - B_k x}}\right) + g(x)_i$, $\forall x \in [x_0, x_i]$
$F(x) \approx \sum_{k=1}^{i} \left(\frac{H_k}{1+2^{A_k - B_k x}}\right)$, $\forall x \in [x_0, x_i]$.
Right limit: $F(x) \approx \sum_{k=1}^{i} H_k, \forall x > x_i$, by induction hypothesis $\lim_{x\to\infty} E(x) = \sum_{k=1}^{i-1} H_k$ and $\lim_{x\to\infty} g(x)_i =$

H_i.
Left limit: $F(x) \approx 0$, $\forall x < x_0$, by induction hypothesis $\lim_{x\to-\infty} E(x) = 0$ and $\lim_{x\to-\infty} g(x)_i = 0$;
Finally, $F(x)$ is defined by the equation (3). □

Corollary 4.1. Given theorem (1), considering that the sigmoidal logistic functions are bijective, and let $F(x)$, let $x_0 < x_1 < x_2 < \cdots < x_n$ be consecutive real numbers determining the intervals of logistic functions $[x_0, x_1]$, $[x_1, x_2]$, ... , $[x_{n-1}, x_n]$. Then, the respective ordinates $[y_0, y_1]$, $[y_1, y_2]$, ... , $[y_{n-1}, y_n]$ are consecutive, and non-overlapping.□

The construction of $F(x)$ extends to other functions $h(x)$, the only condition is that the limits of $h(x)$ as x tends to $\pm\infty$ are constant.

Theorem 2. The coupled model with n functions, each with constant limits as x tends to $\pm\infty$, is:

$$F(x) = h(x)_1 + h(x)_2 + \cdots + h(x)_n, \tag{4}$$

Where $\lim_{x\to-\infty} h(x) = L$, $\lim_{x\to\infty} h(x) = R$, and L and R are constants.
Therefore $\lim_{x\to-\infty} F(x) = K_1$, $\lim_{x\to\infty} F(x) = K_2$, and K_1 and K_2 are constants.□

The proof is similar to Theorem 1. If two or more functions with total or partial intersection of their intervals, that is, they are defined in the same interval, they are added.

Figure 1 shows the coupling of four functions: Gompertz, Logistic, algebraic, and wave function. Only the first two are properly sigmoidal, the third is an algebraic function with sigmoidal behavior, and the last is the wave function. It is possible to include different functions that meet the conditions explained, for example, the normal distribution function.

The function $y = F(x)$ is described by equation (5):

$$y = \underbrace{2 \cdot e^{-e^{2-x}}}_{Gompertz\ f.} + \underbrace{\frac{2}{1+e^{10-x}}}_{Sigmoidal\ f.} + \underbrace{\frac{(x-20)}{\sqrt{1+(x-20)^2}}}_{Algebraic\ function} \underbrace{-4e^{-\frac{(x-30)^2}{4}} sin\left(\frac{x-30}{4}\right)}_{Wave\ function} + 1 \tag{5}$$

The wave function satisfies the requirement of Theorem 2. Proof: By definition $-1 \leq sin(x) \leq 1$, it follows that, $-\frac{1}{e^{x^2}} \leq \frac{sin(x)}{e^{x^2}} \leq \frac{1}{e^{x^2}}$. Since the limits of both functions are equal, $\lim_{x\to\infty} -\frac{1}{e^{x^2}} = \lim_{x\to\infty} \frac{1}{e^{x^2}} = 0$, it follows that $\lim_{x\to\infty} e^{-x^2} sin\,(x) = 0$ (squeeze theorem), and in the same way we can obtain $\lim_{x\to-\infty} e^{-x^2} sin\,(x) = 0$.□

The code to graph $F(x)$ in R is:

```
y = function(x){
 2*e^( -e^(2-x) ) + 2/( 1+e^( 10-x ) ) +
 (x-20)/sqrt( 1+(x-20)^2 ) -
 4*e^(-(x-30)^2/4)*sin((x-30)/4) + 1
}
plot(y, 0, 37, col="green")
```

4.5 The model for COVID-19

First, an efficient sigmoidal function had to be selected. Subsequently, a model for COVID-19 was developed.

The fundamental element of the model is the logistic sigmoidal function, equation (20). Specifically, the model $F(x)$ is a summation of ordered logistic functions, starting with the function $g(x)_1$ for the first wave, $g(x)_2$ for the second wave, and so on up to $g(x)_n$ for the last wave. Then, the model for COVID-19 is a coupled model with sigmoidal functions specified in theorem (1), and is given by equation (6):

$$F(x) = g(x)_1 + g(x)_2 + \cdots + g(x)_n \tag{6}$$

4.6 Empirical execution time

In this section, the time required to estimate the model parameters in each country is calculated.

The experiment was repeated forty times in each country [25], and the average was recorded to avoid bias. Table 7 presents the results; in the case of Italy, the time is higher due to the presence of six waves (one more than the other countries). Subsequently, the mathematical model reported low times.

Table 7: Execution time (in seconds) to calculate the parameters of a logistic model by country

Country	Running time (in seconds)
Italy	0.2968650
Brazil	0.1491925
Switzerland	0.1799175
Peru	0.1215575

4.7 Application of the logistic function to COVID-19

The logistic function $F(x)$ is a set of functions, which are ordered sequentially and do not overlap. Each function corresponds to a wave of COVID-19.

Figure 2 represents the cumulative number of deaths from COVID-19. The dataset (observed data) is represented in gray, and the logistic function $F(x)$ in blue, and the turning points in red. The observed data are very close to the curve. Remark: While the sigmoidal shape of the later waves cannot be distinguished due to the scale (thousands on the ordinate axis), it is visible if these (one or two) waves are plotted exclusively.

In all cases, the first two or three waves were relatively larger and lasted longer (their length on the x-axis is the duration in days); in addition, they had a greater number

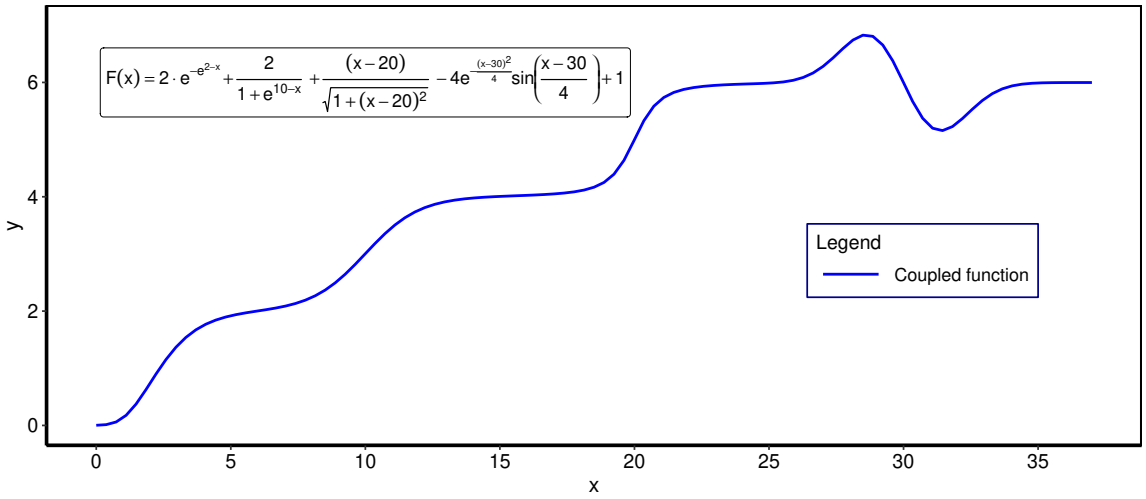

Figure 1: The coupled function $F(x)$ is made up of four functions: Gompertz, Logistic, algebraic, and wave. Only the first two are properly sigmoidal, the third is an algebraic function with sigmoidal behavior, and the last is the wave function.

Table 8: Logistic sigmoidal function adjustment measures

Country	**Pearson Correlation** ρ	**Coefficient of Determination**	**RMSE**	**MAE**	**p-value for** ρ	**Confidence interval for** ρ
Italy	0.9999230	0.999846	0.7164719	0.5779384	$< 2.2 \cdot 10^{-16}$	0.9999150 , 1
Brazil	0.9999283	0.9998566	3.013632	1.99136	$< 2.2 \cdot 10^{-16}$	0.9999208 , 1
Switzerland	0.9999178	0.9998356	0.061266	0.04001958	$< 2.2 \cdot 10^{-16}$	0.9999092 , 1
Peru	0.9999050	0.99981	1.022324	0.6213603	$< 2.2 \cdot 10^{-16}$	0.9998951 , 1
Average	0.9999185	0.9998371	1.203423	0.80767	$< 2.2 \cdot 10^{-16}$	
Std. Dev.	0.00001	0.00002	1.271652	0.832245	$< 2.2 \cdot 10^{-16}$	

of victims (represented by the height on the ordinate axis). Meanwhile, subsequent waves were considerably shorter in duration and had fewer victims. In each country, the last wave ends almost flat (the slope tends to zero); under these circumstances, the pandemic ended. The second wave in Brazil was the largest (it can be observed that it led to more than 400,000 deaths).

The Pearson product-moment correlation coefficients (ρ) were greater than 0.9999 (see the second column in Table 8), indicating very strong positive associations; that is, a high degree of association between the observed data and the function. Moreover, the correlations are statistically significant in the four countries. The p-values ($< 2.2 \cdot 10^{-16}$) are below the significance level of 0.01, and the confidence intervals are presented in column seven.

Brazil and Italy received the best adjustment, while Peru received the worst, but the differences were minimal.

The coefficients of determination (third column) indicate that the models obtained are explained or determined by the differences in the days.

The RMSE is 0.72 in Italy, 3.01 in Brazil, 0.06 in Switzerland, and 1.02 in Peru, and the MAE is 0.58, 1.99, 0.04, and 0.62, respectively. The metrics indicate a low average distance between the model's predicted and dataset values.

F-test: The regression model is statistically significant in the four countries; therefore, the regression model's utility permits the calculation of various estimates and predictions (with p-value $= 2.2 \times 10^{-16}$, less than the significance level of 0.01).

Equations (7), (8), (9), and (10) represent the functions $F(x)$:

$$\underbrace{F(x)}_{Italy} = \frac{34.6}{1+2^{5.77-0.116*x}} + \frac{45.22}{1+2^{25.1-0.087*x}} + \frac{49.77}{1+2^{18.45-0.047*x}} + \frac{35.74}{1+2^{32.57-0.046*x}} + \frac{12.9}{1+2^{43.62-0.049*x}} + \frac{10.51}{1+2^{58.91-0.057*x}} \quad (7)$$

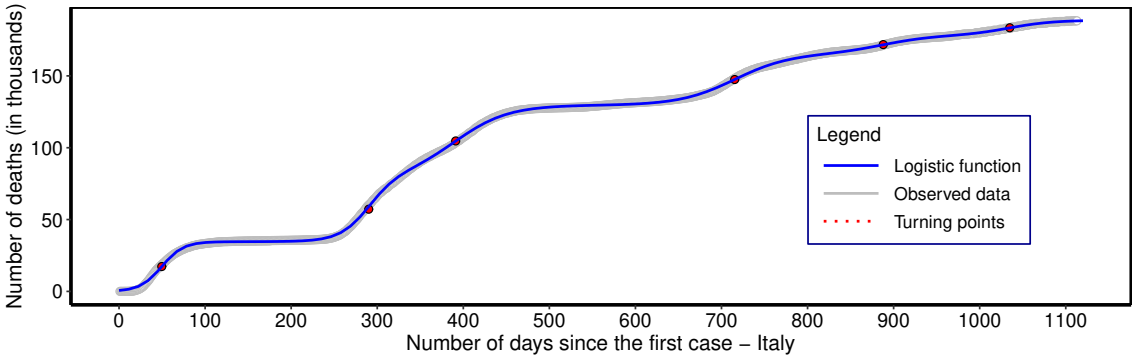

(a) Case: Italy with six waves.

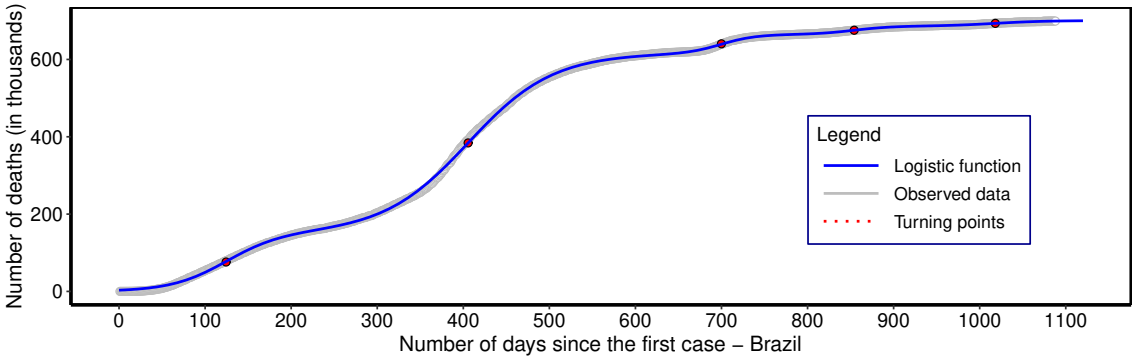

(b) Case: Brazil with five waves.

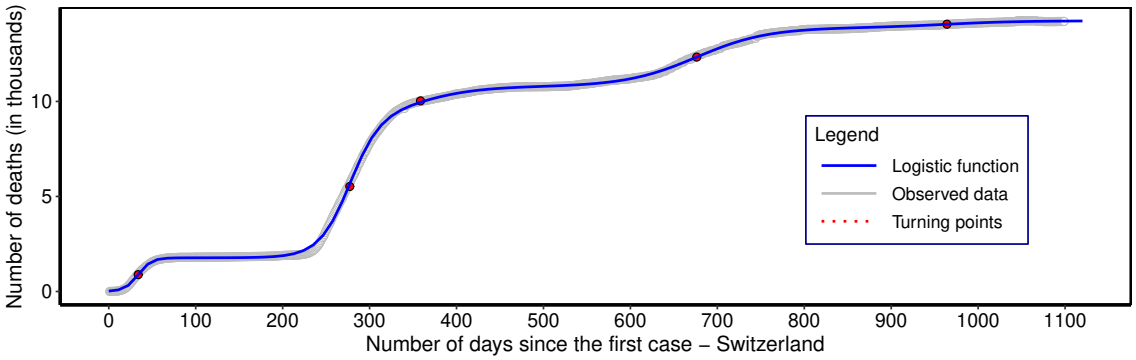

(c) Case: Switzerland with five waves.

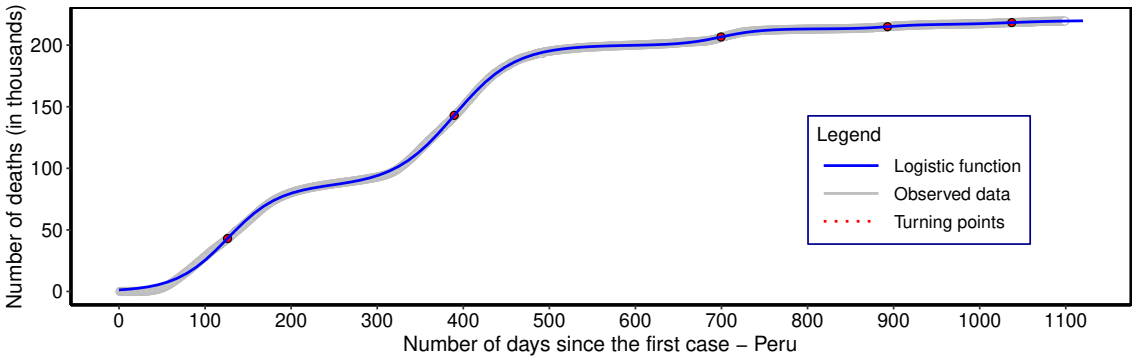

(d) Case: Peru with five waves.

Figure 2: Logistic function of the cumulative number of deaths from COVID-19 (in thousands) by day. The observed data are represented in gray, the logistic function $F(x)$ in blue, and the turning points in red.

$$\underbrace{F(x)}_{Brazil} = \frac{152.06}{1+2^{5.62-0.045*x}} + \frac{464.04}{1+2^{11.9-0.029*x}} + \frac{48.72}{1+2^{51.47-0.074*x}} + \frac{21.45}{1+2^{56.44-0.066*x}} + \frac{14.2}{1+2^{50.35-0.049*x}} \quad (8)$$

$$\underbrace{F(x)}_{\text{Switzerland}} = \frac{1.77}{1+2^{6.49-0.192*x}} + \frac{7.51}{1+2^{22.68-0.082*x}} + \frac{1.5}{1+2^{14.71-0.041*x}} + \frac{3.1}{1+2^{24.01-0.036*x}} + \frac{0.36}{1+2^{33.8-0.035*x}} \quad (9)$$

$$\underbrace{F(x)}_{Peru} = \frac{85.94}{1+2^{6.07-0.048*x}} + \frac{114.1}{1+2^{15.96-0.041*x}} + \frac{13.22}{1+2^{44.35-0.063*x}} + \frac{3.4}{1+2^{73.16-0.082*x}} + \frac{3.33}{1+2^{46.8-0.045*x}} \quad (10)$$

4.8 First derivative

The first derivative of the logistic function $g(x)$ or equation (20) is given in equation (11):

$$g'(x) = \frac{B\,H\,\ln(2)\,2^{A-B\,x}}{\left(1+2^{A-B\,x}\right)^2}, \quad (11)$$

Where x is the number of days since the first case, $g'(x)$ is the death rate of the cumulative number of deaths, H is the height of the wave, A and B are the pandemic constants, and ln is the natural logarithm of base e; that is, $\ln(x) = \log_e(x)$.

The first derivative is helpful as it represents the speed of spread. It is also used to calculate the second derivative.

4.9 Second derivative

Calculating the second derivative is necessary to obtain the turning point

The equation (12) is the second derivative of the logistic function $g(x)$; that is, the derivative of the equation (11):

$$g''(x) = -\frac{B^2\,H\ln(2)^2\,2^{A-Bx}\left(1-2^{A-Bx}\right)}{\left(1+2^{A-Bx}\right)^3}, \quad (12)$$

where x is the number of days since the first, $g''(x)$ is the second derivative (also called the acceleration) of the cumulative number of deaths, H is the height of the wave, and A and B are the pandemic constants.

4.10 Third derivative

The third derivative $F'''(x)$ is:

$$\frac{B^3\,H\ln(2)^3\,2^{A-Bx}\left(1-4\cdot 2^{A-Bx}+2^{2(A-Bx)}\right)}{\left(1+2^{A-Bx}\right)^4}, \quad (13)$$

Where x is the number of days since the first case, the third derivative $g'''(x)$ is the rate of change of acceleration over time (also known as jerk, it is aptly named because a large jerk means a sudden change in acceleration, which causes an abrupt movement), and H is the height of the wave. Finally, A and B are the pandemic constants.

4.11 Turning point

A point c on a curve $y = g(x)$ is called a turning point (or inflection point) if g is continuous and the curve changes from concave to convex (or vice versa) at c.

To obtain the turning point, it is first necessary to find the stationary point of $g'(x)$; that is, to solve the following equation $g''(x) = 0$. Then, the solution is given by $x_0 = \frac{A}{B}$ and $y_0 = \frac{H}{2}$.

Finally, $g'''(x_0)$ is evaluated $F'''(x_0) = -0.0416\,B^3\,H$. The result is different from zero (with $B \neq 0$ and $H \neq 0$), which indicates that $(\frac{A}{B}, \frac{H}{2})$ is a turning point; more calculation details can be found in Appendix A.4.

4.12 Meaning of the turning point

The turning or inflection points are important because they represent moments when the trend of the observed variable changes (mathematically, this is the point where it changes from concave up to concave down). In the context of the pandemic, they indicate a change in the spread of the virus, which can have direct implications for public health policies and governmental interventions. For example, they could be associated with easing mitigation measures (quarantines or social distancing) or healthcare capacity.

4.13 Applying high-order derivatives

We continued by deriving the functions $F(x)$. The results are equations (14), (15), (16), and (17), which represent the first derivatives for Italy, Brazil, Switzerland, and Peru, respectively, using equation (11).

$$\underbrace{F'(x)}_{Italy} = \frac{2.79 \cdot 2^{5.77-0.116*x}}{(1+2^{5.77-0.116*x})^2} + \frac{2.71 \cdot 2^{25.1-0.087*x}}{(1+2^{25.1-0.087*x})^2} + \frac{1.63 \cdot 2^{18.45-0.047*x}}{(1+2^{18.45-0.047*x})^2} + \frac{1.13 \cdot 2^{32.57-0.046*x}}{(1+2^{32.57-0.046*x})^2} + \frac{0.44 \cdot 2^{43.62-0.049*x}}{(1+2^{43.62-0.049*x})^2} + \frac{0.41 \cdot 2^{58.91-0.057*x}}{(1+2^{58.91-0.057*x})^2} \quad (14)$$

$$\underbrace{F'(x)}_{Brazil} = \frac{4.76 \cdot 2^{5.62-0.045*x}}{(1+2^{5.62-0.045*x})^2} + \frac{9.44 \cdot 2^{11.9-0.029*x}}{(1+2^{11.9-0.029*x})^2} + \frac{2.48 \cdot 2^{51.47-0.074*x}}{(1+2^{51.47-0.074*x})^2} + \frac{0.98 \cdot 2^{56.44-0.066*x}}{(1+2^{56.44-0.066*x})^2} + \frac{0.49 \cdot 2^{50.35-0.049*x}}{(1+2^{50.35-0.049*x})^2} \quad (15)$$

$$\underbrace{F'(x)}_{\text{Switzerland}} = \frac{0.24 \cdot 2^{6.49-0.192*x}}{(1+2^{6.49-0.192*x})^2} + \frac{0.43 \cdot 2^{22.68-0.082*x}}{(1+2^{22.68-0.082*x})^2} + \frac{0.04 \cdot 2^{14.71-0.041*x}}{(1+2^{14.71-0.041*x})^2} + \frac{0.08 \cdot 2^{24.01-0.036*x}}{(1+2^{24.01-0.036*x})^2} + \frac{0.01 \cdot 2^{33.8-0.035*x}}{(1+2^{33.8-0.035*x})^2} \quad (16)$$

$$\underbrace{F'(x)}_{Peru} = \frac{2.87 \cdot 2^{6.07-0.048*x}}{(1+2^{6.07-0.048*x})^2} + \frac{3.24 \cdot 2^{15.96-0.041*x}}{(1+2^{15.96-0.041*x})^2} + \frac{0.58 \cdot 2^{44.35-0.063*x}}{(1+2^{44.35-0.063*x})^2} + \frac{0.19 \cdot 2^{73.16-0.082*x}}{(1+2^{73.16-0.082*x})^2} + \frac{0.1 \cdot 2^{46.8-0.045*x}}{(1+2^{46.8-0.045*x})^2} \quad (17)$$

The equation (12) was used to calculate the second derivative of the function $F(x)$.

Finally, the turning points are detailed in Table 9.

4.14 Interpretation

The first derivative of the function $F(x)$ allows us to describe the behavior of the rate or speed of the number of deaths. It provides an elegant and analytically based justification for the term "wave."

Figure 3 shows the graphs of the first $F(x)$ derivatives for each country as blue curves. The turning points of function $F(x)$ are projected onto $F'(x)$ and displayed with red dashed lines. For comparison between waves or countries, both axes have the same scale.

Definition 4.1 (x)**.** The value of the abscissa x is the number of days elapsed since the first case or cases. Then, the range (i.e., the number of days from an initial value x_i to another final value x_j, with $x_i \leq x_j$) is the duration or the number of days ($x_j - x_i + 1$). In a complete wave, the range is its duration in days. The definition extends to higher-order derivatives and their respective graphs.

Definition 4.2 ($F'(x)$)**.** The value of the ordinate $F'(x)$ is the death rate or the change of deaths at x (i.e., on the day x, if $x \in \mathbb{N}$). It is also the velocity of the cumulative number of deaths, indicates the rate at which the number of deaths changes with respect to days. Moreover, if this value is higher than that on another day, it can be immediately understood as indicating higher lethality.

Definition 4.3 ($F''(x)$)**.** The value of the ordinate $F''(x)$ is the change in death rate at x. It is also the acceleration of the cumulative number of deaths at x (i.e., on the day x, if $x \in \mathbb{N}$). The second derivative, with respect to days, gives the acceleration, which describes how the velocity of "the cumulative number of deaths" changes over days.

The first waves in Italy and Switzerland reached a lower death rate and shorter duration, which may be for different reasons, including strict social isolation measures and population differences. In Peru and Brazil, it lasted more than 200 days and had fatality rates below and above one, respectively. Using the proposed model, it was possible to characterize the waves of COVID-19, and it is expected that it can be extended to other countries (which also present similar patterns, according to our pilot study).

Figure 4 represents the graphs of the second derivative of $F(x)$ (for Italy and Brazil only) as blue curves, where the turning points of function F(x) are projected onto F'(x) and displayed with red dashed lines. It can be understood as the acceleration of the cumulative number of deaths due to COVID-19.

Finally, a function $F(x)$ is concave upward in the intervals where its first derivative increases, that is, when the second derivative is positive. Similarly, F(x) is concave downward in the intervals where the second derivative is negative. The second derivatives $F''(x)$ are given by equations (18), and (19).

Table 9: Turning points by country

Wave	Brazil	Italy	Switzerland	Peru
1	124.38	49.65	33.87	126.08
2	405.60	290.09	277.20	389.42
3	699.89	391.13	358.53	699.39
4	854.16	715.31	676.27	892.89
5	1018.16	887.93	964.09	1037.25
6		1034.91		

$$\underbrace{F''(x)}_{Italy} = \frac{0.22 \cdot 2^{5.77-0.116*x}(1-2^{5.77-0.116*x})}{(1+2^{5.77-0.116*x})^3} + \frac{0.16 \cdot 2^{25.1-0.087*x}(1-2^{25.1-0.087*x})}{(1+2^{25.1-0.087*x})^3} + \frac{0.05 \cdot 2^{18.45-0.047*x}(1-2^{18.45-0.047*x})}{(1+2^{18.45-0.047*x})^3} + \frac{0.04 \cdot 2^{32.57-0.046*x}(1-2^{32.57-0.046*x})}{(1+2^{32.57-0.046*x})^3} + \frac{0.01 \cdot 2^{43.62-0.049*x}(1-2^{43.62-0.049*x})}{(1+2^{43.62-0.049*x})^3} + \frac{0.02 \cdot 2^{58.91-0.057*x}(1-2^{58.91-0.057*x})}{(1+2^{58.91-0.057*x})^3} \quad (18)$$

$$\underbrace{F''(x)}_{Brazil} = \frac{0.15 \cdot 2^{5.62-0.045*x}(1-2^{5.62-0.045*x})}{(1+2^{5.62-0.045*x})^3} + \frac{0.19 \cdot 2^{11.9-0.029*x}(1-2^{11.9-0.029*x})}{(1+2^{11.9-0.029*x})^3} + \frac{0.13 \cdot 2^{51.47-0.074*x}(1-2^{51.47-0.074*x})}{(1+2^{51.47-0.074*x})^3} + \frac{0.05 \cdot 2^{56.44-0.066*x}(1-2^{56.44-0.066*x})}{(1+2^{56.44-0.066*x})^3} + \frac{0.02 \cdot 2^{50.35-0.049*x}(1-2^{50.35-0.049*x})}{(1+2^{50.35-0.049*x})^3} \quad (19)$$

5 Discussion

The calculation time of a sigmoid function $g(x)$, depends on the number and type of operations required (in computing, exponentiation is more expensive than multiplication/-division, and these, in turn, are more expensive than addition/subtraction). The logistic sigmoidal function requires one exponentiation operation, one multiplication, one division, and two additions/subtractions. Other functions require an equal or greater number of operations and/or have more costly operations:

- The Boltzmann function has the same number and type of operations (one exponentiation, two divisions, and two additions/subtractions). If division costs more than multiplication, the model would be disadvantaged.
- The hyperbolic tangent function requires six operations (one additional subtraction operation).
- The Gompertz function requires five operations (one additional exponentiation operation).

The minimum number of operations required is five, with at most one exponentiation operation and two multiplication/division operations. Thus, the logistic function is efficient in relation to the set of functions (explained in Table 6).

The coupled mode $F(x)$ consists of a summation of logistic functions. It is defined by equation (3): $F(x) = \sum_{i=1}^{n} \frac{H_i}{1+2^{A_i - B_i x}}$, and has no added elements, although previous works do contain them (described in Table **??**):

- The first work by Vilca Oliver et al. [4] presents models $F(x,q) = \sum_{w=1}^{n} \left(\frac{\prod_{i=1}^{w-1}(i-q)\prod_{j=w+1}^{n}(j-q)}{(n-w)!(-1)^{w-1}(w-1)!} \cdot A_w \cdot e^{-e^{B_w - C_w \cdot x}} \right)$ and $F(x,q) = \sum_{w=1}^{n} \left(\frac{2^{w-1}\&q}{2^{w-1}} \cdot A_w \cdot e^{-e^{B_w - C_w \cdot x}} \right)$ which include an additional variable, q, among other details.
- The model by El Aferni, Ahmed et al. [17] $F(x) = I_{min} + I_{max} \sum_{i=1}^{n} \left(\frac{P_i}{1+10^{(A_i - x)B_i}} \right)$ includes two additional components (I_{min} and I_{max}).
- In the second work by Vilca Oliver et al. [5], en $F(x,q) = \sum_{w=1}^{n} \left(\frac{\prod_{i=1}^{w-1}(i-q)\prod_{j=w+1}^{n}(j-q)}{(n-w)!(-1)^{w-1}(w-1)!} \frac{I_w}{1+e^{\frac{(Z_w - x)}{D_w}}} \right)$ y $F(x,q) = \sum_{w=1}^{n} \left(\frac{2^{w-1}\&q}{2^{w-1}} \frac{I_w}{1+e^{\frac{(Z_w - x)}{D_w}}} \right)$ contain additional elements such as the variable q and others.

Thus, the presented model has a more straightforward structure than its predecessors

On the other hand, the average Pearson correlation coefficient for the logistic sigmoidal models is $\rho_{Logistic} = 0.99992$, and the standard deviation is 0.00001, which explains that they statistically approximate each other.

The coefficients are higher than those in previous works (sigmoidal mathematical models presented in Table **??**, particularly in Peru and Brazil). They are also slightly higher than those for models with ANNs ($\rho_{ANNs} = 0.99991$).

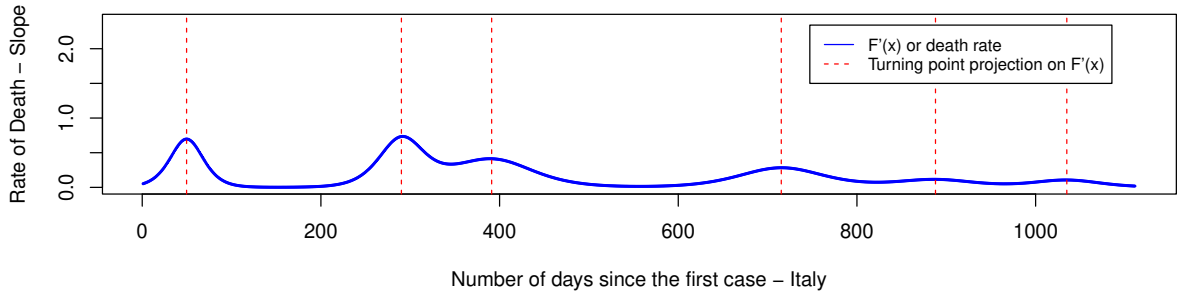

(a) Case: Italy has six waves.

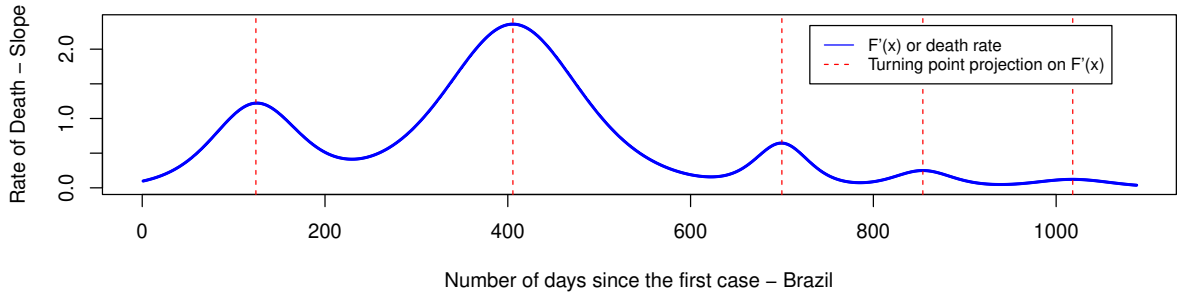

(b) Case: Brazil has five waves, the first and second, with high mortality rates.

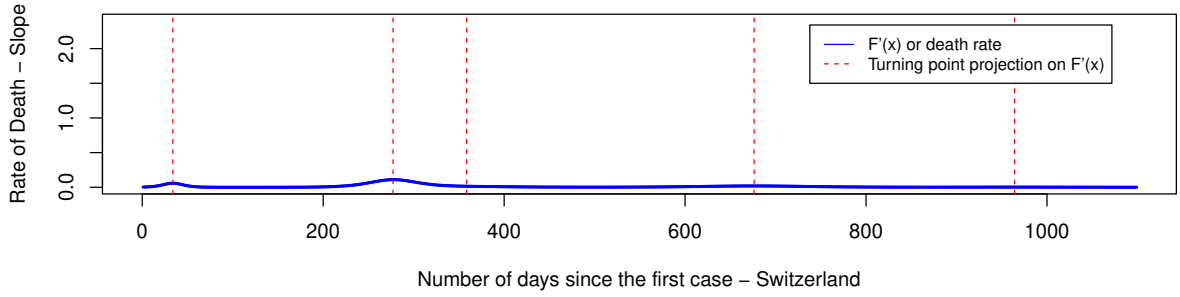

(c) Case: Switzerland has five waves and low death rates.

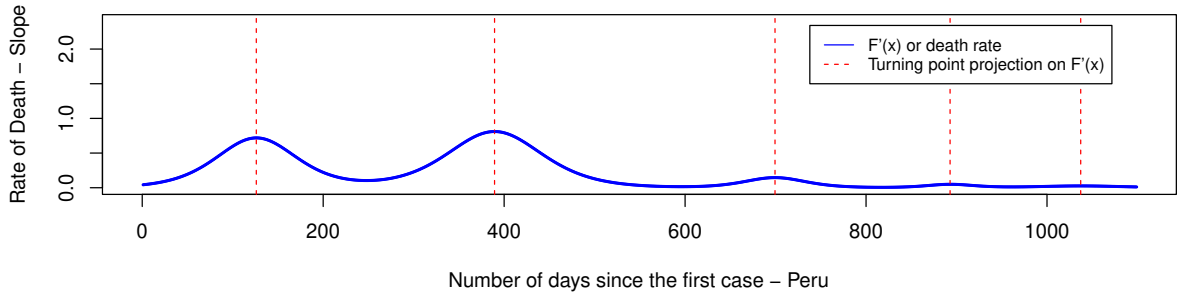

(d) Case: Peru has five waves.

Figure 3: Death rate ($F'(x)$, first derivative of the COVID-19 logistic function of cumulative COVID-19 deaths) in blue, and the vertical projection of the turning points on $F'(x)$ (red dashed line).

Similarly, the Pearson correlation coefficients of the ANN models are greater than or equal to those in previous ANN works (exposed in Table 2).

Regarding the empirical execution time, the sigmoidal model and the ANN are different concepts (mathematical model vs. deep learning). The former requires fewer operations, while the latter includes a more complex architecture (i.e., layers, neurons, and matrix products). Therefore, it is understandable that the sigmoidal models are faster (less than a third of a second; see Table 7).

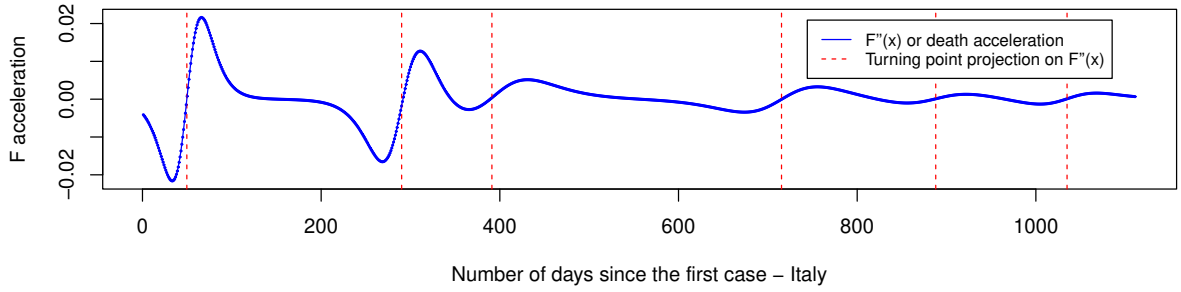

(a) Case: Italy with six waves.

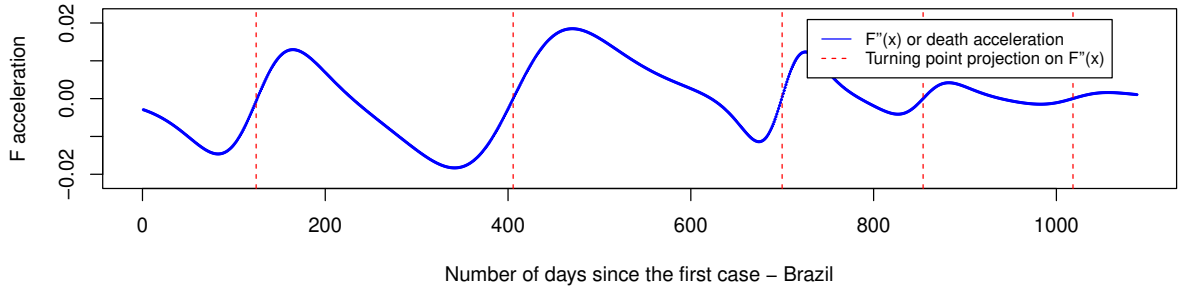

(b) Case: Brazil with five waves.

Figure 4: Death acceleration ($F''(x)$, second derivative of the logistic function of cumulative COVID-19 deaths) in blue, and the projections of the turning points on $F''(x)$ as red vertical dashed lines (Italy and Brazil).

6 Conclusion

In almost all countries, particularly in the study countries (i.e., Italy, Brazil, Switzerland, and Peru), the COVID-19 waves presented a sigmoidal behavior. Therefore, the proposed model obtained high Pearson correlation coefficients.

The logistic function is efficient, as analyzed by the type and quantity of operations. A new version of the logistic function $g(x)$ was obtained and used, without adding operations.

The main contribution of this work is the COVID-19 model that can be used on data that are not necessarily epidemiological and with any function $h(x)$ with constant left and right asymptotes (that is, $\lim_{x\to-\infty} h(x) = L$, and $\lim_{x\to\infty} h(x) = R$, where L and R are constants, proven by mathematical induction).

The first three derivatives of the sigmoidal logistic function were calculated, allowing for a precise and elegant analysis. Moreover, the turning points (i.e., the point at which the concavity of the function changes) were obtained. The derivatives allowed the waves of COVID-19 to be described, analyzed, and compared, as well as providing justification for the well-known term "waves."

Highly representative and expressive sigmoidal logistic functions were obtained, which stand out for their efficiency in running time, far surpassing that of the tested artificial neural network. The function obtained a good fit, as the waves presented sigmoidal behavior which is typical of epidemics.

The ANN can adapt to any curve without the requirement that it presents a specific pattern. Therefore, such a model would be preferable if atypical behaviors were present in the observed data but at the expense of additional time. Also, it is suitable for large data sets and high dimensionality in the input variables.

Finally, neither model is better, and both have advantages and disadvantages. Both are good for modeling epidemics, mainly when the data follow a sigmoidal pattern.

Four real cases were studied, and models and methodologies were developed. Therefore, the procedures can be applied in other countries and to different datasets beyond COVID-19. Finally, they may be helpful for forecasting and modeling in the case of future pandemics or other practical implications.

Funding statement

This research was funded by Universidad Nacional del Altiplano (UNA), IPN SIP 20231387 project (RR. N. 1589-2023-R-UNA)

Conflict of interest

The authors declare no conflicts of interest. The funders had no role in the design of the study; in the collection, analyses, or interpretation of data; in the writing of the manuscript; or in the decision to publish the results.

Acknowledgement

To the administrative staff and the Vice-Rectorate of Research of the Universidad Nacional del Altiplano for their combined efforts and support.

References

[1] S. Kumar, "Monitoring Novel Corona Virus (COVID-19) Infections in India by Cluster Analysis," *Annals of Data Science*, vol. 7, no. 3, pp. 417–425, sep 2020. [Online]. Available: https://doi.org/10.1007/s40745-020-00289-7

[2] M. A. Alsalem, A. H. Alamoodi, O. S. Albahri, K. A. Dawood, R. T. Mohammed, A. Alnoor, A. A. Zaidan, A. S. Albahri, B. B. Zaidan, F. M. Jumaah, and J. R. Al-Obaidi, "Multi-criteria decision-making for coronavirus disease 2019 applications: a theoretical analysis review," *Artificial Intelligence Review*, vol. 55, no. 6, pp. 4979–5062, aug 2022. [Online]. Available: https://doi.org/10.1007/s10462-021-10124-x

[3] N. Pearce, D. A. Lawlor, and E. B. Brickley, "Comparisons between countries are essential for the control of COVID-19," *International Journal of Epidemiology*, vol. 49, no. 4, pp. 1059–1062, jun 2020, _eprint: https://academic.oup.com/ije/article-pdf/49/4/1059/34275473/dyaa108.pdf. [Online]. Available: https://doi.org/10.1093/ije/dyaa108

[4] O. A. Vilca-Huayta and U. Y. Tito, "Efficient function integration and a case study with gompertz functions for covid-19 waves," *International Journal of Advanced Computer Science and Applications*, vol. 13, no. 8, 2022. [Online]. Available: http://dx.doi.org/10.14569/IJACSA.2022.0130863

[5] O. A. Vilca Huayta, A. C. Jimenez Chura, C. B. Sosa Maydana, and A. J. Martínez García, "Analysis of the epidemic curve of the waves of covid-19 using integration of functions and neural networks in peru," *Informatics*, vol. 11, no. 2, 2024. [Online]. Available: https://www.mdpi.com/2227-9709/11/2/40

[6] Z. A. Oraibi and S. Albasri, "Efficient COVID-19 Prediction by Merging Various Deep Learning Architectures," *Informatica*, vol. 48, no. 5, Feb. 2024, number: 5. [Online]. Available: https://www.informatica.si/index.php/informatica/article/view/5424

[7] V. Janko, G. Slapničar, E. Dovgan, N. Reščič, T. Kolenik, M. Gjoreski, M. Smerkol, M. Gams, and M. Luštrek, "Machine learning for analyzing non-countermeasure factors affecting early spread of covid-19," *International Journal of Environmental Research and Public Health*, vol. 18, no. 13, 2021. [Online]. Available: https://www.mdpi.com/1660-4601/18/13/6750

[8] D. Cherifi, A. Djaber, M.-E. Guedouar, A. Feghoul, Z. Z. Chelbi, and A. A. Ouakli, "Covid-19 Detecting in Computed Tomography Lungs Images using Machine and transfer Learning," *Informatica*, vol. 47, no. 8, Sep. 2023. [Online]. Available: https://www.informatica.si/index.php/informatica/article/view/4258

[9] R. Sujath, J. M. Chatterjee, and A. E. Hassanien, "A machine learning forecasting model for COVID-19 pandemic in india," *Stochastic Environmental Research and Risk Assessment*, vol. 34, no. 7, pp. 959–972, 2020. [Online]. Available: https://doi.org/10.1007/s00477-020-01827-8

[10] S. Shastri, K. Singh, S. Kumar, P. Kour, and V. Mansotra, "Time series forecasting of covid-19 using deep learning models: India-usa comparative case study," *Chaos, Solitons and Fractals*, vol. 140, p. 110227, 2020. [Online]. Available: https://www.sciencedirect.com/science/article/pii/S0960077920306238

[11] F. Fernandes, S. F. Stefenon, L. O. Seman, A. Nied, F. C. S. Ferreira, M. C. M. Subtil, A. C. R. Klaar, and V. R. Q. Leithardt, "Long short-term memory stacking model to predict the number of cases and deaths caused by COVID-19," *Journal of Intelligent & Fuzzy Systems*, vol. 42, no. 6, pp. 6221–6234, 2022, publisher: IOS Press.

[12] S. Namasudra, S. Dhamodharavadhani, and R. Rathipriya, "Nonlinear Neural Network Based Forecasting Model for Predicting COVID-19 Cases," *Neural Processing Letters*, vol. 55, no. 1, pp. 171–191, 2023.

[13] F. Özen, "Random forest regression for prediction of Covid-19 daily cases and deaths in Turkey," *Heliyon*, vol. 10, no. 4, p. e25746, 2 2024, publisher: Elsevier. [Online]. Available: https://doi.org/10.1016/j.heliyon.2024.e25746

[14] S. Kanchan, E. Ogden, M. Kesheri, A. Skinner, E. Miliken, D. Lyman, J. Armstrong, L. Sciglitano, and G. Hampikian, "COVID-19 hospitalizations and deaths predicted by SARS-CoV-2 levels in Boise, Idaho wastewater," *Science of The Total Environment*, vol. 907, p. 167742, Jan. 2024. [Online]. Available: https://www.sciencedirect.com/science/article/pii/S0048969723063696

[15] S. Abolmaali and S. Shirzaei, "A comparative study of SIR Model, Linear Regression, Logistic Function and ARIMA Model for forecasting COVID-19 cases," *AIMS Public Health*, vol. 8, no. 4, pp. 598–613, aug 2021. [Online]. Available: https://www.ncbi.nlm.nih.gov/pmc/articles/PMC8568588/

[16] R. A. Conde-Gutiérrez, D. Colorado, and S. L. Hernández-Bautista, "Comparison of an artificial

neural network and Gompertz model for predicting the dynamics of deaths from COVID-19 in México," *Nonlinear Dynamics*, vol. 104, no. 4, pp. 4655–4669, Jun. 2021. [Online]. Available: https://doi.org/10.1007/s11071-021-06471-7

[17] A. El Aferni, M. Guettari, and A. Hamdouni, "COVID-19 multiwaves as multiphase percolation: a general N-sigmoidal equation to model the spread," *The European Physical Journal Plus*, vol. 138, no. 5, p. 393, may 2023. [Online]. Available: https://doi.org/10.1140/epjp/s13360-023-04014-0

[18] J. H. University, "Github - cssegisanddata/covid-19: Novel coronavirus (covid-19) cases, provided by jhu csse." [Online]. Available: https://github.com/CSSEGISandData/COVID-19

[19] M. Haouari and M. Mhiri, "A particle swarm optimization approach for predicting the number of COVID-19 deaths," *Scientific Reports*, vol. 11, no. 1, p. 16587, Aug. 2021. [Online]. Available: https://www.nature.com/articles/s41598-021-96057-5

[20] M. Viková and M. Vik, "Transition Temperature of Color Change in Thermochromic Systems and Its Description Using Sigmoidal Models," *Materials*, vol. 16, no. 23, p. 7478, jan 2023, number: 23 Publisher: Multidisciplinary Digital Publishing Institute. [Online]. Available: https://www.mdpi.com/1996-1944/16/23/7478

[21] L. Mei, "Model Construction of Higher Education Quality Assurance System Based on Fuzzy Neural Network," *Informatica*, vol. 48, no. 10, Jun. 2024, number: 10. [Online]. Available: https://www.informatica.si/index.php/informatica/article/view/5676

[22] S. F. Ardabili, A. Mosavi, P. Ghamisi, F. Ferdinand, A. R. Varkonyi-Koczy, U. Reuter, T. Rabczuk, and P. M. Atkinson, "Covid-19 outbreak prediction with machine learning," *Algorithms*, vol. 13, no. 10, 2020. [Online]. Available: https://www.mdpi.com/1999-4893/13/10/249

[23] N. P. Dharani and P. Bojja, "Analysis and Prediction of COVID-19 by using Recurrent LSTM Neural Network Model in Machine Learning," *International Journal of Advanced Computer Science and Applications (IJACSA)*, vol. 13, no. 5, 2022. [Online]. Available: https://thesai.org/Publications/ViewPaper?Volume=13&Issue=5&Code=IJACSA&SerialNo=21

[24] M. H. Oukhouya, N. Angour, N. Aboutabit, and I. Hafidi, "Comparative Analysis of ARDL, LSTM, and XGBoost Models For Forecasting The Moroccan Stock Market During The COVID-19 Pandemic," *Informatica*, vol. 49, no. 14, Mar. 2025. [Online]. Available: https://www.informatica.si/index.php/informatica/article/view/5751

[25] O.-A. Vilca and M.-C. Rivara, "Study on the Average Size of the Longest-Edge Propagation Path for Triangulations," Feb. 2025, pp. 368–375. [Online]. Available: https://www.scitepress.org/Link.aspx?doi=10.5220/0009162703680375

[26] G. Gu, P. Zhang, S. Chen, Y. Zhang, and H. Yang, "Inflection point: a perspective on photonic nanojets," *Photonics Research*, vol. 9, no. 7, pp. 1157–1171, july 2021, publisher: Optica Publishing Group. [Online]. Available: https://opg.optica.org/prj/abstract.cfm?uri=prj-9-7-1157

[27] Y. A. Hong and J. W. Ha, "Enhanced refractive index sensitivity of localized surface plasmon resonance inflection points in single hollow gold nanospheres with inner cavity," *Scientific Reports*, vol. 12, no. 1, p. 6983, apr 2022, number: 1 Publisher: Nature Publishing Group. [Online]. Available: https://www.nature.com/articles/s41598-022-11197-6

[28] I. Bronshtein, K. Semendyayev, G. Musiol, and H. Mühlig, *Handbook of Mathematics*. Berlin, Heidelberg: Springer, 2015. [Online]. Available: https://link.springer.com/10.1007/978-3-662-46221-8

A Appendix

The logistic sigmoidal function:

$$g\left(x\right)=\frac{H}{1+2^{A-Bx}} \tag{20}$$

For derivatives the following abbreviated notation is used:

$$g'(x)=\frac{\mathrm{d}}{\mathrm{d}x}\left[g(x)\right]=\left[g(x)\right]'$$

A.1 First derivative

The first derivative is given in the equation (21):

$$\begin{aligned}
g'\left(x\right) &= H\cdot\left[\tfrac{1}{1+2^{A-Bx}}\right]',\ pull\ out\ constant\ factors\\
g'\left(x\right) &= -H\cdot\tfrac{\left[1+2^{A-Bx}\right]'}{\left(1+2^{A-Bx}\right)^{2}},\ apply\ the\ reciprocal\ rule\\
g'\left(x\right) &= -\frac{H\left(\ln\left(2\right)\cdot 2^{A-Bx}\cdot\left[A-Bx\right]'+0\right)}{\left(1+2^{A-Bx}\right)^{2}}\\
g'\left(x\right) &= \frac{B\,H\,\ln\left(2\right)\,2^{A-B\,x}}{\left(1+2^{A-B\,x}\right)^{2}}
\end{aligned} \tag{21}$$

A.2 Second derivative

The equation (22) is the second derivative of the logistic function $g(x)$:

$$\begin{aligned} g''(x) &= B\,H\,\ln(2)\left[\frac{2^{A-B\,x}}{\left(1+2^{A-B\,x}\right)^2}\right]', \\ &\quad pull\ out\ constant\ factors \\ g''(x) &= B\,H\,\ln(2)\cdot \\ &\quad \left[\frac{\left[2^{A-Bx}\right]'\left(1+2^{A-Bx}\right)^2-2^{A-Bx}\left[\left(1+2^{A-Bx}\right)^2\right]'}{\left(\left(1+2^{A-B\,x}\right)^2\right)^2}\right]', \\ &\quad apply\ the\ quotient\ rule \\ g''(x) &= -\frac{B^2\,H\ln(2)^2\,2^{A-Bx}\left(1-2^{A-Bx}\right)}{\left(1+2^{A-Bx}\right)^3} \end{aligned} \tag{22}$$

A.3 Third derivative

The third derivative $g'''(x)$ is:

$$B\,H\,\ln(2)\left[-\frac{B^2\,H\ln(2)^2\,2^{A-Bx}\,\left(1-2^{A-Bx}\right)}{\left(1+2^{A-Bx}\right)^3}\right]', \quad pull\ out\ constant\ factors$$

Applying the quotient rule and simplifications as in the second derivative:

$$\frac{B^3\,H\ln(2)^3\,2^{A-Bx}\,\left(1-4\cdot\,2^{A-Bx}+2^{2\,(A-Bx)}\right)}{\left(1+2^{A-Bx}\right)^4} \tag{23}$$

The same results were obtained using the GNU Octave software (version 9.1.0) with the following code:

Listing 1: Octave code for derivatives

```
pkg load symbolic;
syms x;
syms A;
syms B;
syms H;
Fx =  H./(1+2^(A-B.*x));

fprintf("First derivative\n");
d1 = diff(Fx,x);
r1 = simplify(factor(d1))
disp(d1);

fprintf("Second derivative:\n");
d2 = diff(d1,x);
r2 = simplify(factor(d2));
disp(r2);

fprintf("Third derivative\n");
d3 = diff(d2,x);
r3 = simplify(factor(d3));
disp(r3);
```

A.4 Turning point

A stationary point of a function is a point where the derivative of a function is equal to zero. The slope of the graph of the function is zero. They are called stationary points because they are points where the function is neither increasing nor decreasing.

A point c on a curve $y = g(x)$ is called a turning point if g is continuous and the curve changes from concave to convex (or vice versa) at c [26, 27].

According to the Method of Higher Derivatives (differential calculus), to obtain the turning point, it is first necessary to find the stationary point of $g'(x)$; that is, to solve the following equation:

$$g''(x) = 0,$$

or

$$-\frac{B^2\,H\ln(2)^2\,2^{A-Bx}\,\left(1-2^{A-Bx}\right)}{\left(1+2^{A-Bx}\right)^3} = 0 \tag{24}$$

The solution to the equation (24) is given by $x_0 = \frac{A}{B}$ and $y_0 = \frac{H}{2}$.

Finally, $g'''(x_0)$ is evaluated as follows:

$$\begin{aligned} F'''(x_0) &= -\frac{B^3\,H\ln(2)^3}{8}, \\ F'''(x_0) &= -0.0416\,B^3\,H. \end{aligned} \tag{25}$$

The result is different from zero (with $B \neq 0$ and $H \neq 0$), which indicates that $(\frac{A}{B}, \frac{H}{2})$ is a turning point. It should be highlighted that, according to the method of Higher Derivatives, if $F''(x_0) = 0$ holds, then x_0 must be substituted into the third derivative. Then, if $F'''(x_0) \neq 0$ holds, then it is a turning point. The method is explained and demonstrated in mathematics books [28].

B Appendix

Listing 2: ANN source code

```
library(tensorflow)
library(keras)
library(ggplot2)
library(devtools)
library(timetk)
library(mlbench)
library(dplyr)
library(magrittr)
library(gridExtra)
library(Metrics) # rmse, mae

 Pais <- 3
 CountryEn <- c("Brazil","Italy"
                ,"Peru","Switzerland")
 File = CountryEn[Pais];
```

```
f2<-paste("Covid19",File,".csv",sep="")
mydata<-read.csv(f2,header=TRUE
                 ,stringsAsFactors=FALSE
                 ,sep=",")
x  <- mydata$x;
y  <- mydata$y;
max_x <- max(x)
max_y <- max(y)
x_dias<-scale(x,center=mean(x)
              ,scale=sd(x))
ym <- mean(y)
ys <- sd(y)
y_train_arr <- (y-ym)/ys
lstm_model <- list()
lstm_model <-
  keras_model_sequential() %>%
  layer_lstm(units=200
             ,return_sequences=TRUE
             ,input_shape=c(1,1)) %>%
  layer_dense(units = 1)

lstm_model %>%
  compile(loss='mae'
          ,optimizer='adam'
          ,metrics=list('mae'))

start.time <- Sys.time()
lstm_model %>% fit(
  x = x_dias, y = y_train_arr,
  batch_size = 1,
  validation_split = 0.05,
  epochs = 500
)
end.time <- Sys.time();
time <- round(end.time - start.time,7);
print(time)

fitted0<- lstm_model %>%
  predict(x_dias,batch_size=1,verbose=0)
fitted <- fitted0*ys + ym
fitted <- round(fitted)

plot(x,y,col="grey",pch=2
     ,xlim=c(0,max_x),ylim=c(0,max_y))
par(new=TRUE)
plot(x,fitted,type="l",col="blue",lwd=5
     ,ylab="",main="",xlab=""
     ,xlim=c(0,max_x),ylim=c(0,max_y))

rc <- cor.test(fitted,y);
print(rc);
rc$estimate[[1]]
rc$estimate[[1]]^2
rc$conf.int[1]
rc$conf.int[2]
rmse(fitted0,y_train_arr)
mae(fitted0,y_train_arr)
```